SPANDIDOS PUBLICATIONS EXPERIMENTAL AND THERAPEUTIC MEDICINE 17: 4344-4356, 2019

Xenotransplantation of human dental pulp stem cells in platelet-rich plasma for the treatment of full-thickness articular cartilage defects in a rabbit model

RICARDO HIDEKI YANASSE[1], ROGER WILLIAM DE LÁBIO[1], LEONARDO MARQUES[2], JOSIANNE TOMAZINI FUKASAWA[1], ROSIMEIRE SEGATO[1], ANGELA KINOSHITA[2], MARIZA AKEMI MATSUMOTO[2], SERGIO LUIS FELISBINO[3], BRUNO SOLANO[4], RICARDO RIBEIRO DOS SANTOS[4] and SPENCER LUIZ MARQUES PAYÃO[1,2]

[1]Department of Genetics, Blood Center, Faculdade de Medicina de Marília (FAMEMA), Marília; [2]Department of Health Sciences, Universidade do Sagrado Coração, Bauru; [3]Department of Morphology, Universidade Estadual Paulista Júlio de Mesquita Filho (UNESP), Botucatu, SP 17519-050; [4]Center for Biotechnology and Cell Therapy, Monte Tabor Hospital São Rafael, Salvador, BA 17519-050, Brazil

Received April 12, 2017; Accepted March 9, 2018

DOI: 10.3892/etm.2019.7499

Abstract. Stem cells in platelet-rich plasma (PRP) scaffolds may be a promising treatment for cartilage repair. Human dental pulp stem cell (hDPSC) subpopulations have been identified to have substantial angiogenic, neurogenic and regenerative potential when compared with other stem cell sources. The present study evaluated the potential of hDPSCs in a PRP scaffold to regenerate full-thickness cartilage defects in rabbits. Full-thickness articular cartilage defects were created in the patellar groove of the femur of 30 rabbits allocated into three experimental groups: Those with an untreated critical defect (CTL), those treated with PRP (PRP) and those treated with stem cells in a PRP scaffold (PRP+SC). The patellar grooves of the femurs from the experimental groups were evaluated macroscopically and histologically at 6 and 12 weeks post-surgery. The synovial membranes were also collected and evaluated for histopathological analysis. The synovial lining cell layer was enlarged in the CTL group compared with the PRP group at 6 weeks (P=0.037) but not with the PRP+SC group. All groups exhibited low-grade synovitis at 6 weeks and no synovitis at 12 weeks. Notably, macroscopic grades for the area of articular cartilage repair for the PRP+SC group were significantly improved compared with those in the CTL (P=0.001) and PRP (P=0.049) groups at 12 weeks. Furthermore, histological scores (modified O'Driscoll scoring system) of the patellar groove articular cartilage in the PRP+SC and PRP groups, in which the articular cartilage was primarily hyaline-like, were significantly higher compared with those in the CTL group at 12 weeks (P=0.002 and P=0.007, respectively). The present results support the therapeutic use of hDPSCs for the treatment of full-thickness articular cartilage defects.

Correspondence to: Dr Ricardo Hideki Yanasse, Department of Genetics, Blood Center, Faculdade de Medicina de Marília (FAMEMA), Rua Lourival Freire 240, Marília, SP 17519-050, Brazil
E-mail: ricardoyanasse@yahoo.com.br

Key words: cartilage, dental pulp, knee, platelet-rich plasma, stem cells

Introduction

Stem cells have inherent chondrogenic potential and serve an important role in healing articular cartilage defects (1). Bone marrow stem cells, which may be obtained by stimulation techniques and by subchondral drilling, have been demonstrated to improve the cartilage healing process; however, these methods result in a fibrocartilage-like tissue that deteriorates over time (2). Other techniques, including autologous chondrocyte implantation, have been used to improve the quality of the repaired tissue to make it more similar to hyaline-like cartilage tissue (3). However, long-term follow-up has identified similar results in terms of clinical outcome and histological scoring between microfracture and autologous chondrocyte implantation techniques (3).

During articular cartilage repair, paracrine factors may influence the inflammatory process involved in fibrocartilage tissue formation. Hyaluronic acid, stem cells and growth factors (GFs) have provided important results with regards to the suppression of inflammatory process (4) and may act synergistically in cartilage regeneration (5,6). Notably, experimental cartilage repair studies have demonstrated promising results when combining subchondral drilling with postoperative intraarticular injections of autologous bone marrow aspirate and hyaluronic acid (4). Synovitis and synovial fluid alterations as a response to the inflammatory process has also been indicated to influence the articular environment and may affect cartilage repair (7).

The use of platelet-rich plasma (PRP), a rich source of autologous GFs, may be considered a useful approach for cartilage repair (8). Platelets serve a crucial role in the normal healing response of connective tissues through the local secretion of GFs and recruitment of reparative cells (9). PRP is a potential scaffold option for tissue regeneration: It has been suggested for the stimulation of chondrogenic differentiation and proliferation of stem cells, chondrocyte proliferation and cartilage formation (10-12).

The type of stem cell may influence the quality of tissue repair (13). Human dental pulp stem cell (hDPSC) subpopulations have been demonstrated to have substantial angiogenic, neurogenic and regenerative potential when compared with other stem cell sources (14,15).

The purpose of the present study was to evaluate the potential of hDPSCs in a PRP scaffold to regenerate full-thickness articular cartilage defects in rabbits. It was hypothesized that hDPSCs in a PRP scaffold may improve articular cartilage repair.

Materials and methods

A total of 32 New Zealand male rabbits (obtained from the Department of coordinating production and maintenance of rabbits, Serviço de Biotério, Prefeitura do Campus da USP (Universidade de São Paulo) (aged 4-6 months, weighing ~3 kg) were used in the present study. Rabbits were maintained in standardized individual cages, at a temperature of ~21˚C, a humidity of 45-55% and a 12-14/24 h light/dark cycle. Additionally, rabbits and received *ad libitum* access to ground solid rations (Anderson and Clayton S.A.) and water. A total of 30 rabbits comprised the experimental group (60 knees), and 2 rabbits were used to obtain PRP. The study protocol of the present experiment was reviewed and approved by the Ethics Committee at Faculdade de Medicina de Marília, São Paulo, Brazil (EC No. 641/12).

hDPSC isolation and culture. Dental pulp cells were extracted from one tooth that had been previously selected for exodontia from a healthy 10 year old female patient at a private dental clinic, on June 2006 (16). Cells were extracted using endodontic files under a biosafety hood and placed in culture flasks with Dulbecco's modified Eagle's medium (DMEM) supplemented with 10% fetal bovine serum (Cultilab, Campinas, SP, Brazil) and 50 mg/ml gentamicin at 37˚C in an atmosphere containing 5% CO_2 as previously described by Jesus *et al* (2011) (16). The growth medium was changed every 3 days. Once cells reached confluence, the cells were dissociated with 0.25% trypsin (Gibco, Thermo Fisher Scientific, Inc., Waltham, MA, USA). Some of the cells were separated for cryopreservation. A maximum of 10^6-10^7 cells per tube were observed and a final volume of 1 ml was then achieved through the addition of DMEM medium supplemented with 10% fetal bovine serum 900 μl (cat. no. 12657029; Gibco; Thermo Fisher Scientific, Inc.) and dimethyl sulfoxide (100 μl; Sigma-Aldrich; Merck KGaA, Darmstadt, Germany). Cryopreservation tubes were then subjected to cryostat reduction for 24 h at -80˚C and then stored in liquid nitrogen (-196˚C). The procedures were performed in the Center for Biotechnology and Cell Therapy, Monte Tabor Hospital São Rafael (Salvador, Brazil).

Flow cytometry. Adherent cells in the sixth passage (P6) and cultures with 60% confluence were selected for the detection of surface and intracellular antigens. Antibody staining was performed as follows: Cell aliquot (100 μl) containing at least 10^6 nucleated cells were placed into each tube and incubated for 30 min at room temperature with 0.5% PBS/BSA (Sigma-Aldrich, Merck KGaA) for blocking. Samples were then stained with conjugated antibodies (all 1:100) for 15 min at room temperature in the dark. Subsequently cells were resuspended twice in 4 ml PBS (Sigma-Aldrich) and centrifuged at a speed of 540 x g for 5 min at 4˚C. Following centrifugation, the supernatant was discarded and the cell pellet was ressuspended in 500 μl PBS + 0.5% BSA and stored at 4˚C. The antibodies used are listed in Table I. Data acquisition and analysis were performed using a FACS Calibur flow cytometer (BD Biosciences) and the Cell Quest program version 5.2 (BD Biosciences). At least 50,000 events were collected and analyzed. Unlabeled antibodies cells were used as controls.

Immunofluorescence. hDPSCs from P6 were used for phenotypic characterization using immunofluorescence. Cells were trypsinized and seeded in 24-well plates containing 13 mm glass coverslips (Waldemar Knittel Glasbearbeitungs GmbH, Braunschweig, Germany). Following adherence for 24 h, the culture medium was removed and two washes with PBS were performed. Cells were fixed with 4% paraformaldehyde for 20 min at room temperature. Two wells were then washed with PBS for 3 min. For the staining of nuclear antigens, cells were permeabilized with 0.1% Triton X-100 for 10 min at room temperature. Blocking was then performed with 5% PBS/BSA (Sigma-Aldrich) for 30 min at room temperature and incubated overnight at 4˚C with the following primary antibodies: Anti-CD44 (1:100; cat. no. 08-0184; Zymed; Thermo Fisher Scientific, Inc.), anti-cluster of differentiation (CD)45 (1:100; cat. no. AHS4552; BioSource; Thermo Fisher Scientific, Inc.) anti-CD90 (1:100; cat. no. 550402; BD Bioscences), anti-CD105 (1:100; cat. no. 555690; BD Bioscences) anti-CD73 (1:100; cat. no. 550738; BD Bioscences), anti-CD117 (1:100; cat. no. ab16832; Abcam, Cambridge, MA, USA), anti-CD133 (1:25; cat. no. ab19898; Abcam) anti-myosin (1:100; cat. no. M7523; Sigma-Aldrich), anti-collagen type I (1:50; cat. no. sc-8788; Santa Cruz Biotechnology Inc., Dallas, TX, USA), anti-glial fibrillary acidic protein (1:50; cat. no. Z0334; Dako; Agilent Technologies, Inc., Santa Clara, CA, USA) and anti-myelin (1:100; cat. no. 18-0038; Zymed; Thermo Fisher Scientific, Inc.). Slides were visualized and images were captured using a confocal microscope (magnification, x400; FluoView 1000; Olympus, Tokyo, Japan).

Cytogenetic analysis. hDPSCs were prepared for cytogenetic analysis as previously described and analyzed using the G-banding technique (17). Slides were observed using an optical microscope (magnification, x1,000) and ~20 metaphases of each sample were analyzed for the presence of numerical and/or structural cytogenetic abnormalities according to the International System for Chromosome Nomenclature (18). Images were captured using Image-Pro Plus software, version 7.0 (Media Cybernetics, Inc., Rockville, MD, USA).

Table I. List of antibodies used for flow cytometry.

Antibody	Source	Supplier/cat. no.
CD44-FITC	Mouse clone L178	BD Biosciences, San Jose, CA, USA/347943
CD90-FITC	Mouse clone 5E10	BD Biosciences, San Jose, CA, USA/555595
CD73-PE	Mouse clone AD2	BD Biosciences, San Jose, CA, USA/550257
CD34-PE	Mouse clone 8G12	BD Biosciences, San Jose, CA, USA/348057
CD45-APC	Mouse clone 2D1	BD Biosciences, San Jose, CA, USA/340942
CD105-FITC	Mouse clone 166707	R&DSystems, Inc., Minneapolis, MN, USA/FAB10971F
CD117-PE-CY5	Mouse clone YB5.B8	BD Biosciences, San Jose, CA, USA/559879
CD133-PE	Mouse monoclonal	Miltenyi/120-000-425
CD166-PE	Mouse clone 3A6	BD Biosciences, San Jose, CA, USA/559263
CD54-PE-CY5	Mouse clone HA58	BD Biosciences, San Jose, CA, USA/555512
STRO-1	Mouse monoclonal	R&DSystems, Inc., Minneapolis, MN, USA/MAB1038
CD31- FITC	Mouse clone WM59	BD Biosciences, San Jose, CA, USA/555445

CD, cluster of differentiation; PE, phycoerythrin; FITC, fluorescein isothiocyanate; APC, allophycocyanin.

All cells obtained from P5 and P6 demonstrated a normal female karyotype (karyotype: 46, XX) (18).

Obtaining and preparing PRP. PRP was obtained from 2 adult New Zealand rabbits (age, 4-6 months; weight, ~3-5 kg). The animals underwent general anesthesia by administering an intramuscular injection of 10 mg/kg xylazine hydrochloride (VET Brands International, Inc., Miramar, FL, USA) followed by an intramuscular injection of 30 mg/kg ketamine hydrochloride (VET Brands International, Inc.). Animals were deemed to be anesthetized when the following parameters were observed: The presence of muscular paralysis, the absence of reflexes and pain. These animals were not used in the experimental groups and following blood extraction, rabbits were euthanized with an overdose (20 mg/kg) of Propofol (Cristália Produtos Químicos Farmacêuticos Ltda., Itapira, São Paulo, Brazil) administered by intravenous injection. Death was confirmed by the lack of a heartbeat, lack of respiration, lack of corneal reflex and the presence of rigor mortis. Cardiac puncture and blood extraction were performed with a 10-ml disposable syringe containing 1 ml 3.2% sodium citrate and a 30x8 mm needle. A total of 9 ml of arterial blood was collected in each syringe and a total of 18 ml of arterial blood was obtained to prepare the PRP. Following collection, the blood was homogenized and transferred to collection tubes (BD Vacutainer; BD Biosciences).

The collected tubes containing the blood were subjected to two centrifugation steps, the first of which was performed at 200 x g for 10 min at 24˚C to separate the blood cells. The supernatant plasma and buffy coat were transferred to a new sterile tube and underwent a second centrifugation step at 400 x g for 10 min at 24˚C. The collected plasma underwent a further centrifugation step at 400 x g for 10 min at 24˚C to concentrate the platelets to ~1,000,000 per μl. Subsequently, the supernatant was removed to achieve a final volume of 1,600 μl of PRP for every 9 ml of arterial blood. PRP was separated into two 800-μl aliquots, placed into sterile cryotubes and stored in a freezer at -80˚C for subsequent experiments. A sample was obtained for platelet counting, which was performed manually using a hemocytometer (Hausser Scientific, Horsham, PA, USA) and was used as a control in order to ensure the minimum concentration of platelets was 1,000,000 per μl.

Prior to the surgical procedure, *hDPSCs* were grown in α-MEM medium (Gibco; Thermo Fisher Scientific, Inc.) supplemented with 10% fetal bovine serum (Gibco; Thermo Fisher Scientific, Inc.) at 37˚C and 5% CO_2 until 80% confluent cultures were obtained. Cells were then detached from the growth surface with 0.25% trypsin (Gibco; Thermo Fisher Scientific, Inc.) and immediately transferred to a tube containing α-MEM medium (supplemented with 10% fetal bovine serum. Samples were centrifuged twice at 175 x g for 10 min at room temperature and the supernatant was removed. Then, PRP was thawed completely, homogenized, divided into 200-μl samples and added to $2{,}8x10^6$ hDPSCs (P5 and P6). The PRP thawing procedure and preparation of the cells was synchronized with the start of surgery and maintained for approximately 10-15 min at room temperature (23-25˚C).

Cell viability. hDPSCs were suspended in PRP and stained with blue tripan reagent (1.6%; v/v; Sigma-Aldrich; Merck KGaA; cat. no. T6146) for 1 min at room temperature and cell viability of ~80% was confirmed by the manual counting technique using a hemocytometer (Hausser Scientific, Horsham, PA, USA).

Surgical procedure and experimental groups. Rabbits received general anesthesia with of 10 mg/kg intramuscular xylazine hydrochloride (Vet Brands International, Inc., Miramar, FL, USA) followed by an intramuscular injection of 30 mg/kg ketamine hydrochloride (Vet Brands International, Inc., Miramar, FL, USA). Each rabbit's right and left knees were shaved and the overlying fur was removed. Antisepsis was performed with 10% polyvinylpyrrolidone topical solution (RioquímicaIndústria Farmaceutica, São José do Rio Preto, Brazil). An incision was made on the anteromedial section of

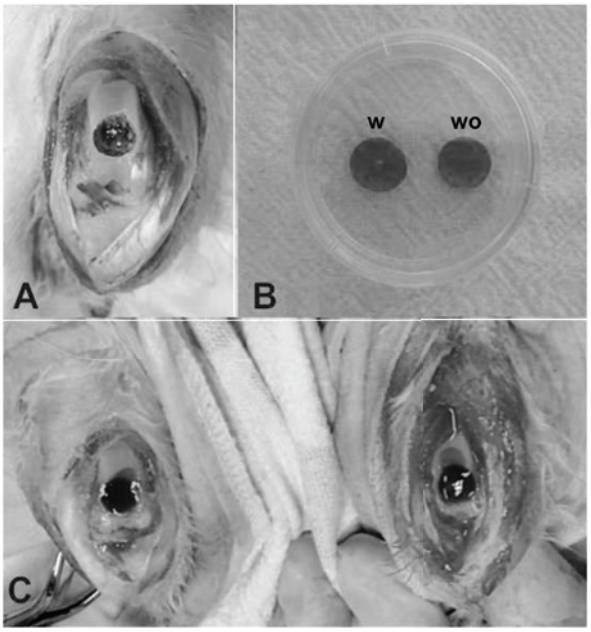

Figure 1. Surgical procedure. (A) Macroscopic view of the full-thickness defect in the trochlear groove of the femur. (B) View of PRP gel scaffold with (w) and without (wo) stem cells. (C) Macroscopic view of the defects filled with PRP gel scaffold with and without stem cells. PRP, platelet-rich plasma.

the knees and the patella was dislocated laterally to expose the patellar groove of the femur. Full-thickness cartilage defects (5x5 mm) down to the subchondral bone were created in the patellar groove using an odontologycal surgical motor for dental implants (Gnatus Produtos Médicos e Odontológicos Ltda EPP, São Paulo, Brazil) quipped with a 5-mm diameter trephine drill and constant irrigation with 0.9% saline solution (Fig. 1A).

Rabbits were allocated into three experimental groups: Control (CTL), PRP and PRP with stem cells (PRP+SC) groups. Both knees of each rabbit were operated on and the 5 mm critical defects were created. In the CTL group, the defects received no further treatment. In the PRP group, the defects in both knees were filled with 100 μl of PRP gel activated with 10% calcium gluconate (Fresenius Kabi Brasil Ltda, Barueri, São Paulo, Brazil). In the PRP+SC group, the defects in both knees were filled with $1.4x10^6$ hDPSCs resuspended in 100 μl of PRP gel activated with 10% calcium gluconate (Fig. 1B and C). The patella was carefully repositioned and the capsule and skin were closed with 4-0 nylon sutures in all of the operated knees. In each group, 5 rabbits were euthanized at 6 weeks and 5 were euthanized at 12 weeks post-surgery.

Macroscopic evaluation. Macroscopic evaluation of cartilage repair was performed at 6 and 12 weeks by two independent observers. The International Cartilage Repair Society (ICRS) evaluation grading system was used as indicated in Table II (19,20).

Histological cartilage evaluation. The distal femur was removed, placed in 10% formalin, decalcified in EDTA, embedded in paraffin and sagittally cut into 5-μm thick sections. Sections were stained with hematoxylin and eosin (H&E) and a Masson-Goldner kit was used for histomorphometric tissue analysis. The microscopic evaluations were performed by two different researchers and scored according to a modified version of the grading system developed by O'Driscoll (21,22), as indicated in Table III. The investigators who performed the evaluations were blind to the treatment.

Table II. International Cartilage Repair Society macroscopic evaluation of cartilage repair.

Variable	Score
Degree of defect repair	
In level with surrounding cartilage	4
75% repair of defect depth	3
50% repair of defect depth	2
25% repair of defect depth	1
0% repair of defect depth	0
Integration to border zone	
Complete integration with surrounding cartilage	4
Demarcating border <1 mm	3
3/4 of graft integrated, 1/4 with a notable border >1 mm in width	2
1/2 of graft integrated with surrounding cartilage, 1/2 with a notable border >1 mm	1
From no contact to 1/4 of graft integrated with surrounding cartilage	0
Macroscopic appearance	
Intact smooth surface	4
Fibrillated surface	3
Small, scattered fissures or cracks	2
Several small or few large fissures	1
Total degeneration of grafted area	0
Total overall repair assessment	
Grade I: Normal	12
Grade II: Nearly normal	8-11
Grade III: Abnormal	4-7
Grade IV: Severely abnormal	1-3

Histology of the synovial membrane. Synovial membrane samples were collected from the lateral parapatellar region for analysis when the animals were euthanized at 6 and 12 weeks. The synovial membrane was placed in 10% formalin at room temperature for 24 h and subsequently embedded in paraffin, sectioned at a thickness of 5 μm and stained with H&E at room temperature for 15 min. The specimens were evaluated by two independent observers using a conventional photonic microscope at a magnification of x40 (Olympus BX41; Olympus Corporation, Tokyo, Japan). The sections were each allocated a Krenn's synovitis score (23), the details of which are indicated in Table IV. A slice of each sample was examined according to the scores and the mean and median scores were calculated for each group.

Statistical analysis. The mean values, standard deviations and medians were obtained for each group. The Kruskall-Wallis

Table III. O'Driscoll's microscopic histological evaluation of articular cartilage.

Variable	Score
Tissue morphology	
Mostly hyaline cartilage	4
Mostly fibrocartilage	3
Mostly non-cartilage	2
Exclusively non-cartilage	1
Matrix staining	
None	1
Slight	2
Moderate	3
Strong	4
Structural integrity	
Severe disintegration	1
Cysts or disruption	2
No organization of chondrocytes	3
Beginning of columnar organization of chondrocytes	4
Normal, similar to healthy mature cartilage	5
Chondrocyte clustering in implant	
25-100% of cells clustered	1
<25% of cells clustered	2
No clusters	3
Intactness of calcified layer; tidemark formation	
<25% of calcified layer intact	1
25-49% of calcified layer intact	2
50-75% of calcified layer intact	3
76-90% of calcified layer intact	4
Complete intactness of calcified cartilage layer	5
Subchondral bone formation	
No formation	1
Slight	2
Strong	3
Histological assessment of surface architecture	
Severe fibrillation of disruption	1
Moderate fibrillation or irregularity	2
Slight fibrillation or irregularity	3
Normal	4
Histological assessment of defect filling	
<25%	1
26-50%	2
51-75%	3
76-90%	4
91-110%	5
Lateral integration of implanted material	
Not bonded	1
Bonded at one hand/partially at both ends	2
Bonded at both sides	3
Basal integration of implanted material	
<50%	1
50-70%	2
70-90%	3
91-100%	4
Inflammation:	
No inflammation	1
Slight inflammation	3
Strong inflammation	5
Maximum total score	45

test was used to determine statistical significance in the differences between the three groups' Krenn synovitis score, the modified O'Driscoll score and the ICRS score, respectively. In cases where this test exhibited significant differences among the three groups, the Kruskall Wallis post-hoc multiple comparisons of mean ranks of all pairs of groups, with Bonferroni's correction was applied. $P<0.05$ was used to indicate a statistically significant difference. The software used for statistical analysis was performed using the Statistica 8.0. software [STATISTICA (data analysis software system) version 8.0. www.statsoft.com; TIBCO software, Inc., Palo Alto, CA, USA].

Results

Macroscopic analysis at 6 weeks. The CTL group exhibited irregular tissue repair with several fissures, and in some knees the defect was not completely filled. The PRP group revealed irregularly repaired cartilage with several fissures that were thinner compared with the surrounding cartilage. Furthermore, in some specimens the center of the defect still had the subchondral bone exposed. Notably, the PRP+SC group demonstrated more regular tissue repair that was level with the surrounding cartilage and exhibited small fissures. At 6 weeks, the PRP+SC group grades were significantly improved compared with those of the PRP group ($P=0.003$; Table V). However, the PRP group exhibited a lower score compared with the CTL group, though this difference was not statistically significant ($P=0.31$).

Macroscopic analysis at 12 weeks. Tissue repair in the CTL group did not significantly improve at 12 weeks post-surgery and the group exhibited irregular tissue repair with several fissures and partial border integration. The PRP group was notably improved and tissue repair was more level with the surrounding cartilage, with small fissures and partial border integration. Furthermore, the PRP+SC group revealed smoother surface cartilage repair that was level with the surrounding cartilage and almost complete border integration. At 12 weeks, the macroscopic grades of the PRP+SC group were significantly improved compared with those of the CTL and the PRP group ($P=0.001$ and $P=0.049$, respectively; Table V).

Histological cartilage evaluation

CTL group. A total of 6 weeks following the surgical procedure, the defects were filled with a thick mixture of hyaline-like and fibrocartilaginous tissue in addition to viable

Table IV. Krenn's synovitis score.

Variable	Score
Enlargement of the synovial lining cell layer	
The lining cells form one layer	0
The lining cells form 2-3 layers	1
The lining cells form 4-5 layers, few multinucleated cells might occur	2
The lining cells form >5 layers, the lining might be ulcerated and multinucleated cells might occur	3
Density of the resident cells	
The synovial stroma shows normal cellularity	0
The cellularity is slightly increased	1
The cellularity is moderately increased, multinucleated cells might occur	2
The cellularity is greatly increased, multinucleated giant cells, pannus formation and rheumatoid granulomas might occur	3
Inflammatory infiltrate	
No inflammatory infiltrate	0
Few mostly perivascular situated lymphocytes or plasma cells	1
Numerous lymphocytes or plasma cells, sometimes forming follicle-like aggregates	2
Dense band-like inflammatory infiltrate or numerous large follicle-like aggregates	3
Total overall assessment	
Sum, 0 or 1	No synovitis
Sum, 2-4	Low-grade synovitis
Sum, 5-9	High-grade synovitis

Table V. Macroscopic evaluation scoring.

	International cartilage repair society score mean ± standard deviation				
Follow-up Period	CTL group	PRP group	PRP + SC group	Kruskal-Wallis P-value	Kruskall Wallis post-hoc multiple comparison with Bonferroni's correction P-value
6 weeks	6.67±3.01	3.60±2.37	8.86±1.35	0.0040[a]	CTL x PRP, P=0.308 CTL x PRP+SC, P=0.516 [a]PRP x PRP+SC, P=0.003
12 weeks	5.50±2.22	7.22±1.92	9.88±0.99	0.0007[a]	CTL x PRP, P=0.549 [a]CTL x PRP+SC, P=0.001 [a]PRP x PRP+SC, P=0.049

[a]P<0.05. CTL, control group without treatment; PRP, group treated with platelet-rich plasma; PRP + SC, group treated with platelet-rich plasma plus human dental pulp stem cells.

cells. Some irregularities were indicated on the surface. No cellular or tissue organization was noted and there was no distinction between the cartilaginous, calcified cartilage and subchondral bone zones. The zone corresponding to the calcified zone sometimes exhibited continuity with fibrous connective tissue; in other cases, this zone exhibited continuity with the mineralized bone remodeling matrix. Furthermore, highly vascularized tissue was above the bone marrow region, which was composed of large blood vessels and occasional sites of clustered inflammatory mononuclear cell infiltrate. In the majority of cases, one of the edges of the defects was not continuous with the adjacent normal cartilage and was occasionally interspersed with fibrous connective tissue or gaps revealing bare bone surface (Fig. 2).

At 12 weeks, the defects were primarily filled with fibrocartilage. Cellular distribution was disorganized, cells were predominantly viable and the surface exhibited irregularities. The majority of the samples exhibited a gap in the central region of the defect. Furthermore, the subchondral bone in the more central portions were replaced by highly vascularized connective tissue. In some samples, there was abnormal mineralization of cartilage in the focal points outside of the

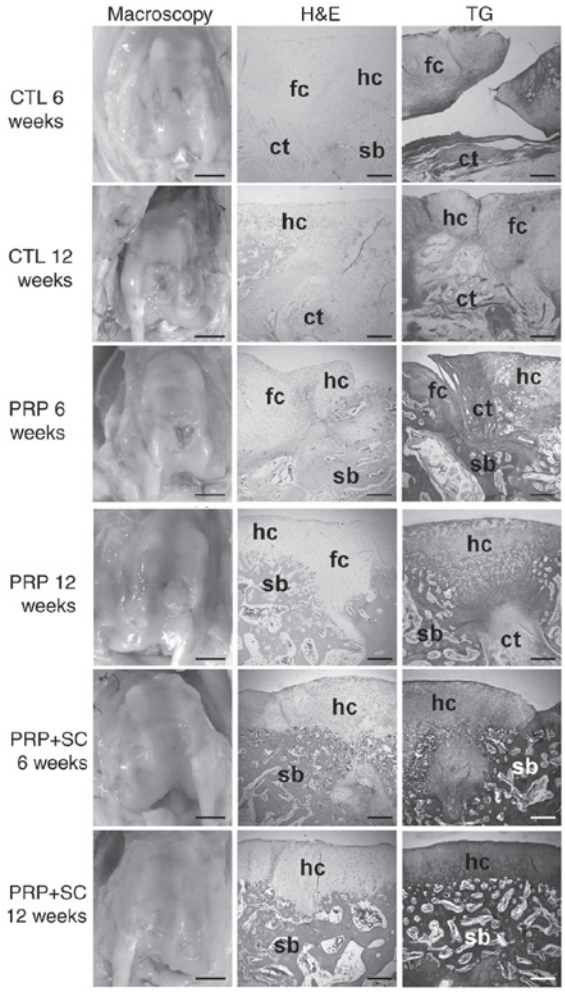

Figure 2. Representative general histology of the articular cartilage defects of the experimental groups stained using hematoxylin and eosin (H&E) and Goldner trichrome (TG). In macroscopy images, scale bars=5 mm. In histological sections, scale bars=200 μm. CTL, control group without treatment; PRP, group treated with platelet-rich plasma; PRP+SC, group treated with PRP plus human dental pulp stem cells; fc, fibrocartilaginous tissue; hc, hyaline cartilage; ct, connective tissue; sb, subchondral bone.

calcification zone. Partial continuity of the repaired cartilage with the normal adjacent cartilage was observed.

PRP group. A total of 6 weeks following the surgical procedure, the defects were filled with a mixture of hyaline-like and fibrocartilaginous tissue, in addition to disorganized viable cells. The surface exhibited fibrillation and irregularities. Notably, improved subchondral bone remodeling was observed. There was also partial continuity with the adjacent normal cartilage (Fig. 2).

At 12 weeks, the defects were filled mostly with hyaline-like cartilage and the surface exhibited fibrillation and irregularities. On the border of the defect, some areas demonstrated features similar to those of normal cartilage organization with regular bone trabeculae, whereas in the center of the defect, thicker cartilage had begun to exhibit columnar cell organization with increased subchondral bone remodeling. In some samples, the subchondral bone was replaced by fibrous connective tissue. There was partial continuity with the adjacent normal cartilage (Fig. 2).

PRP+SC group. At 6 weeks, the defects were predominantly filled with hyaline-like cartilage. Cellular distribution was disorganized, cells were viable and the surface was moderately smooth. In the subchondral region, half of the samples exhibited fibrous connective tissue with areas of granulation without continuity and with the bone corresponding to the central region of the defect. Islands of cartilage were observed amid the medullary bone in the region corresponding to the defect. In some cases, granulation tissue or foci of calcification were identified to be interposed in the cartilaginous layer. Notably, there was partial continuity with the adjacent normal cartilage (Fig. 2).

At 12 weeks, the defects were predominantly filled with hyaline-like cartilage and early signs of columnar cell organization were apparent. The surface was smooth and lamina splendens were present. Bone trabeculae in the subchondral region were regular and in the process of remodeling. Furthermore, lateral integration with the adjacent normal cartilage partially occurred in the majority of the defects (Fig. 2).

As indicated in Table VI, histological scoring assessment at 6 weeks demonstrated that the PRP+SC group had a significantly higher mean score compared with the CTL group regarding the histological assessment of surface architecture and lateral integration of implanted material (P=0.0009 and P=0.0069, respectively). Regarding histological assessment of surface architecture, the PRP group exhibited no significant differences with the CTL group. Furthermore, the PRP+SC group exhibited a significantly higher score compared with the PRP group regarding the histological assessment of surface architecture and lateral integration of implanted material (P=0.0148 and P=0.0059, respectively).

As indicated in Table VII, at 12 weeks the PRP+SC group was indicated to have a significantly higher mean histological evaluation score compared with the CTL group for the following variables: Tissue morphology, matrix staining, chondrocyte clustering in implant, histological assessment of surface architecture, subchondral bone formation and total score (P=0.0037, P=0.0172, P=0.0323, P=0.0006, P=0.0465 and P=0.0021, respectively; Table VII). Additionally, the PRP group scores were higher compared with those of the CTL group in the cases of tissue morphology, matrix staining, intactness of calcified layer and tidemark formation, histological assessment of surface architecture, subchondral bone formation and total score (P=0.0363, P=0.0024, P=0.0132, P=0.0209, P=0.0323 and P=0.0076, respectively; Table VII). There were no significant differences between the PRP+SC group and the PRP group.

Synovial membrane microscopic morphological analysis using Krenn's synovitis scoring. At 6 weeks, the synovial membranes of all three groups exhibited loose connective tissue with slightly increased cellularity and were permeated by discrete perivascular lymphocytic inflammatory infiltrate (Fig. 3). Furthermore, the layer of synovial lining cells was enlarged in the CTL group and consisted of two to three smaller cell layers. Conversely, the PRP and PRP+SC groups typically exhibited a single layer of synovial lining cells. As indicated in Table VIII, the enlargement of the synovial lining cell layer was significantly increased in the CTL group when

Table VI. Histological evaluation at 6 weeks.

Variable	Mean ± standard deviation			Kruskal-Wallis P-value	Kruskall Wallis post-hoc multiple comparison with Bonferroni's correction P-value
	CTL group	PRP group	PRP + SC group		
Tissue morphology	3.83±0.41	3.50±0.53	3.86±0.38	0.216	-
Matrix staining	3.83±0.41	3.40±0.70	3.86±0.38	0.193	-
Structural integrity	4.0±0.00	3.60±0.52	4.00±0.00	0.050	-
Chondrocyte clustering in implant	2.00±0.00	1.80±0.42	2.43±0.53	0.025[a]	CTL x PRP, P=1,000 CTL x PRP+SC, P=0.699 PRP x PRP+SC, P=0.155
Intactness of calcified layer, formation of tidemark	1.17±0.41	1.90±1.10	1.57±0.53	0.280	-
Subchondral bone formation	2.00±0.00	2.40±0.52	2.29±0.49	0.222	-
Histological assessment of surface architecture	2.00±0.00	2.50±0.53	3.86±0.38	<0.001[a]	CTL x PRP, P=0.675 [a]CTL x PRP+SC, P=0.001 [a]PRP x PRP+SC, P=0.015
Histological assessment of defect filling	4.83±0.41	4.50±0.53	5.00±0.00	0.065	-
Lateral integration of implanted material	2.00±0	2.10±0.32	3.00±0	<0.001[a]	CTL x PRP, P=1.000 [a]CTL x PRP+SC, P=0.007 [a]PRP x PRP+SC, P=0.006
Basal integration of implanted material	3.00±0	3.50±0.53	3.43±0.79	0.156	-
Inflammation: Maximum total score	1.00±0	1.40±0.84	1.00±0	0.256	-
Total score	29.67±1.03	30.60±4.30	34.29±1.60	0.047[a]	CTL x PRP, P=1,000 CTL x PRP+SC, P=0.062 PRP x PRP+SC, P=0.164

[a]P<0.05. CTL, control group without treatment; PRP, group treated with platelet-rich plasma; PRP + SC, group treated with platelet-rich plasma plus human dental pulp stem cells.

compared with the PRP group (P=0.037) and had a tendency to be increased when compared with the PRP+SC group. In addition, a low degree of synovitis was identified in all three groups at 6 weeks (Table VIII).

At 12 weeks, the three groups exhibited normal cellularity and no evident inflammation. The layer of synovial lining in the CTL group continued to be comprised of two to three smaller cell layers and the PRP and PRP+SC groups exhibited a normal single layer; however, the difference between the synovitis evaluation scoring in these groups was not statistically significant. Notably, no synovitis was indicated in any of the three groups at 12 weeks (Fig. 3; Table VIII).

Discussion

A primary advantage of mesenchymal stem cells (MSCs) is their capacity to differentiate into osteocytes and chondrocytes, and their ability to regenerate cartilage and the underlying subchondral bone essential for adequate healthy cartilage support (24). The use of stem cells in articular cartilage repair is promising, and has been demonstrated to enhance repair; however, its experimental application through intraarticular MSC injections may result in fibrocartilaginous tissue formation (25). This outcome reflects the fact that other factors are involved in adequate cell differentiation and tissue repair (24-28).

Synovial fluid serves a key role in osteoarthritis by allowing for different tissue communication inside the joint in multidirectional pathways (29,30). In cases of osteoarthritis, the synovial fluid is a predominant source of extrinsic signaling factors and proinflammatory cytokines, and there is an increased number of MSCs present (31). This increase in MSCs in the synovial fluid and the cases of synovitis with infiltration of inflammatory cells in the synovium maybe interpreted as responses to inflammation and tissue injury. It has been reported that signaling molecules contribute to cartilage repair involving the synovial fluid and the calcified cartilage of the subchondral bone, which allows for these locations to interact as functional units (32).

In the present study, synovial analysis revealed low-grade synovitis at 6 weeks in all groups and decreased synovitis at 12 weeks. Although the degree of synovitis was similar between the groups, the CTL group exhibited pronounced enlargement of the synovial lining layer, which persisted at 12 weeks. This finding validated the interaction and signaling of tissue repair with the synovium after the creation of the defect and raises the question whether the synovium and synovial fluid should also be targeted to improve cartilage tissue repair. A previous experimental study on rabbits indicated multiple joint injections of PRP to be beneficial in reducing synovitis and inflammatory factors and in restoring damaged

Table VII. Histological evaluation at 12 weeks.

Variable	Mean ± standard deviation			Kruskal-Wallis P-value	Kruskall Wallis post-hoc multiple comparison with Bonferroni's correction P-value
	CTL group	PRP group	PRP + SC group		
Tissue morphology	3.10±0.32	3.78±0.44	4.0±0.00	0.003[a]	[a]CTL x PRP, P=0.036 [a]CTL x PRP+SC, P=0.004 PRP x PRP+SC, P=1.000
Matrix staining	2.90±0.32	3.89±0.33	3.75±0.46	0.002[a]	[a]CTL x PRP, P=0.002 [a]CTL x PRP+SC, P=0.017 PRP x PRP+SC, P=1.000
Structural integrity	3.30±0.95	4.22±0.67	4.38±0.52	0.020[a]	CTL x PRP, P=0.163 CTL x PRP+SC, P=0.073 PRP x PRP+SC, P=1.000
Chondrocyte clustering in implant	1.80±0.42	2.00±0.50	2.63±0.52	0.007[a]	CTL x PRP, P=1.000 [a]CTL x PRP+SC, P=0.032 PRP x PRP+SC, P=0.172
Intactness of calcified layer, formation of tidemark	1.30±0.48	2.67±1.12	2.25±0.71	0.005[a]	[a]CTL x PRP, P=0.013 CTL x PRP+SC, P=0.069 PRP x PRP+SC, P=1.000
Subchondral bone formation	2.20±0.42	2.89±0.33	2.88±0.35	0.002[a]	[a]CTL x PRP, P=0.032 [a]CTL x PRP+SC, P=0.046 PRP x PRP+SC, P=1.000
Histological assessment of surface architecture	1.70±0.48	2.89±0.78	3.38±0.52	<0.001[a]	[a]CTL x PRP, P=0.021 [a]CTL x PRP+SC, P=0.001 PRP x PRP+SC, P=0.816
Histological assessment of defect filling	4.80±0.42	5.00±0.00	5.00±0.00	0.171	-
Lateral integration of implanted material	2.20±0.42	2.22±0.44	2.50±0.53	0.335	-
Basal integration of implanted material	3.80±0.42	3.89±0.33	3.25±0.46	0.013[a]	CTL x PRP, P=1.000 CTL x PRP+SC, P=0.146 PRP x PRP+SC, P=0.076
Inflammation maximum total score	1.00±0.00	1.00±0.00	1.00±0.00	1.000	-
Total score	28.10±2.56	34.44±3.88	35.00±2.27	0.001[a]	[a]CTL x PRP, P=0.008 [a]CTL x PRP+SC, P=0.002 PRP x PRP+SC, P=1.000

[a]P<0.05. CTL, control group without treatment; PRP, group treated with platelet-rich plasma; PRP + SC, group treated with platelet-rich plasma plus human dental pulp stem cells.

tissue (7). In addition, PRP has been demonstrated to stimulate cell proliferation and superficial zone protein secretion by articular cartilage and synovium in the human knee joint (33). The mechanisms of action in PRP therapy are complex, multifaceted and remain to be fully elucidated. However, in osteoarthritis, PRP has been suggested to exhibit pro-anabolic or anti-catabolic mechanisms and to provide pain relief (29). In the present study, although the difference was not statistically significant, the PRP and PRP+SC groups exhibited reduced synovitis at 6 and 12 weeks compared with the respective CTL groups. However, further study is warranted to determine whether synovitis maybe attenuated by PRP or stem cells, and thus influence cartilage repair.

MSCs differ in their chondrogenic potential. When the synovial fluid, synovium, bone marrow, adipose tissue and muscle MSCs were compared, those of the synovial fluid, synovium and bone marrow exhibited improved chondrogenic potential (13,34,35). The present study examined hDPSCs because hDPSC subpopulations have been demonstrated to have higher angiogenic, neurogenic and regenerative potential compared with bone marrow stem cells or adipose stem cells (14). The chondrogenic potential of hDPSCs has not been compared to that of other MSCs; however several *in vitro* and *in vivo* studies have suggested hDPSCs as a promising tool for cartilage repair (15,36,37), which was corroborated by the present study.

A review of *in vitro* studies has indicated a positive interaction between PRP and MSCs with regards to stimulation of stem cell proliferation, the lack of interference with lineage differentiation, preservation of multipotency and

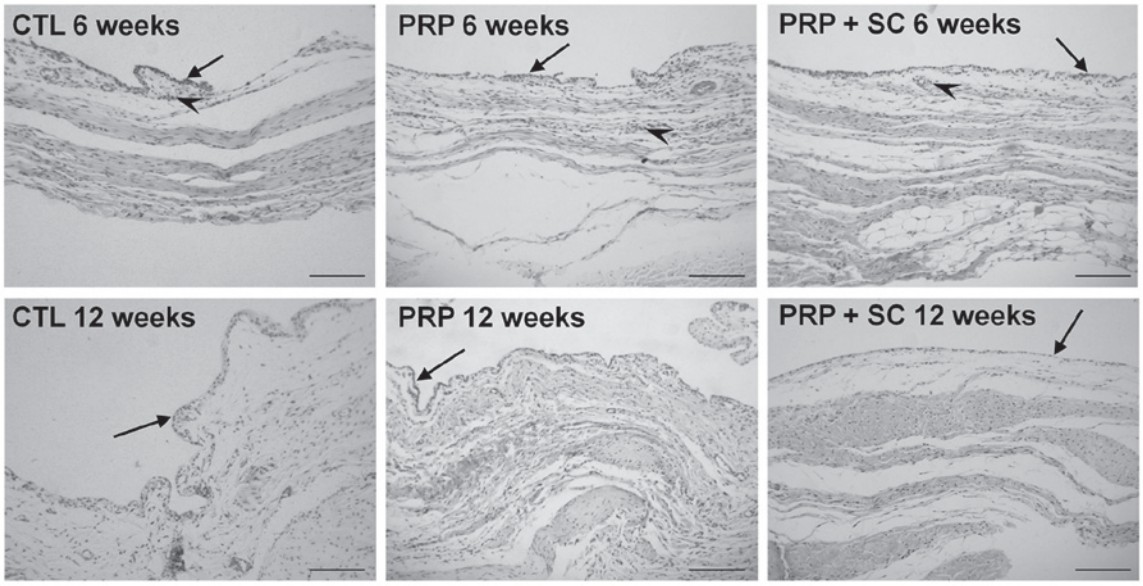

Figure 3. Representative view of synovial membrane histology from experimental groups stained using H&E. Arrows indicate the layer of synovial lining cells with some stratification in all groups at 6 weeks post-surgery. Inflammatory infiltrate was minimal and was only observed surrounding the blood vessels at 6 weeks post-surgery (arrow heads). Scale bars=100 μm. CTL, control group without treatment; PRP, group treated with platelet-rich plasma; PRP+SC, group treated with PRP plus human dental pulp stem cells.

the immune-privileged characteristics of the MSCs and the delay of the development/emergence of the senescent phenotype (38). In the case of articular cartilage repair, a review has demonstrated that PRP may stimulate chondrogenic differentiation *in vitro* and enhance cartilage repair in animal studies (39). Notably, PRP has diverse compositions, concentrations and activation methods, which produce conflicting results on its effects on cartilage repair (40,41). Carneiro *et al* (42) reported the use of autologous PRP gel with the presence of leukocytes concentrated two to three times in a full-thickness cartilage defect in an ovine model. The study indicated improved results after 12 weeks, though the repair did not consist of hyaline cartilage. Serra *et al* (43) reported the use of multiple injections of autologous PRP in a full-thickness defect in a rabbit model and observed no differences in repair relative to controls after 19 weeks. Additionally, Milano *et al* (22,44) reported a positive effect of PRP on cartilage repair after microfractures and identified the effect to be more pronounced when PRP was mixed with fibrin glue and used as a gel in comparison with a liquid intraarticular injection; however, hyaline cartilage formation was not observed (22). The PRP gel scaffold used in the present study was homologous and contained leukocytes, which may influence the hDPSCs and autologous bone marrow cells present in the defect (45).

In the present study, the use of PRP gel containing hDPSCs at the defect site contributed to improved subchondral bone formation, with repaired tissue consisting primarily of hyaline-like cartilage. In addition, a smooth articular cartilage surface was indicated. By contrast, the CTL group exhibited a more irregular and fibrillated articular cartilage surface and the repaired tissue consisted mostly of fibrocartilage. Notably, the full-thickness cartilage defect created in the present study allowed exposure of the subchondral bone. As a result, a more pronounced migration of bone marrow cells can occur, which promotes interaction with the PRP and the hDPSCs (46). This type of interaction may be useful in a surgical intervention for cartilage repair but requires further exploration.

The present results indicated that, in the PRP and PRP+SC groups the formation of a homogeneous calcified cartilage and tidemark was improved compared with the CTL group, particularly on the border of the defect. Furthermore, the quality of the adjacent repaired cartilage was also improved. In all three groups, the center of the defect still had signs of subchondral bone remodeling in which vascularized connective tissue was present, particularly in the CTL group. The findings of the present study suggest that adequate subchondral bone formation and remodeling seem to be fundamental for restoring and obtaining high quality repaired cartilage. Notably, a 12-week follow-up period is short and differences in subchondral bone and any gaps in healed cartilage may likely be more pronounced at 24 weeks (47).

The lamina splendens consists of collagen fibrils that run parallel to the surface of the joint (48). It is responsible for maintaining the mechanical response of the articular cartilage to load absorption and is the first component to degrade in osteoarthritis (49). If the surface zone layer and adequate superficial zone protein (lubricin) are not reestablished, their loss may lead to the ultimate failure of any articular cartilage repair as a result of the shear forces in the joint (49). In the present study, smoother cartilage surfaces were observed in the PRP and PRP+SC groups and the repaired cartilage of the PRP+SC group had the majority of its surface layer covered by lamina splendens. This finding suggests that the cartilage repaired in the PRP+SC group may resist longer and more adequately to heavier loads. It was speculated that this end point may be particularly important and that further histological analyses are required in cartilage repair studies.

Table VIII. Synovitis evaluation scoring.

Follow-up period	Groups	Enlargement of the synovial lining cell layer			Density of the resident cells		Inflammatory infiltrate			Sum of Krenn's synovitis score		Synovitis grade
		Mean (SD)	Kruskall Wallis (P-value)	Post hoc test with Bonferroni correction	Mean (SD)	Kruskall Wallis (P-value)	Mean (SD)	Kruskall Wallis (P-value)	Kruskall Wallis post-hoc multiple comparison with Bonferroni correction	Mean (SD)	Kruskall Wallis (P-value)	
6 weeks	CTL	1.17 (0.41)	0.017[a]	[a]CTL x PRP, P=0.037	0.83 (0.41)	0.622	0.83 (0.41)	0.835	-	2.83 (0.75)	0.107	Low
	PRP	0.30 (0.67)		CTL x PRP+SC, P=0.200	0.90 (0.32)		0.70 (0.48)			1.80 (1.14)		Low
	PRP+SC	0.43 (0.53)		PRP x PRP+SC, P=1.000	0.71 (0.49)		0.71 (0.49)			1.86 (0.90)		Low
12 weeks	CTL	0.70 (0.48)	0.007[a]	CTL x PRP, P=0.067	0.20 (0.42)	0.174	0.00 (0.00)	0.005[a]	CTL x PRP, P=0.171	0.90 (0.74)	0.096	No
	PRP	0.10 (0.32)		CTL x PRP+SC, P=0.120	0.50 (0.53)		0.50 (0.53)		CTL x PRP+SC, P=1.000	1.10 (0.99)		No
	PRP+SC	0.13 (0.35)		PRP x PRP+SC, P=1.000	0.13 (0.35)		0.00 (0.00)		PRP x PRP+SC, P=0.218	0.25 (0.46)		No

[a]P<0.05. CTL, control group without treatment; PRP, group treated with platelet-rich plasma; PRP + SC, group treated with platelet-rich plasma plus human dental pulp stem cells; SD, standard deviation.

The present study had some limitations. The follow-up period was too short to definitively understand the outcome or the lasting effects of the repaired cartilage. In addition, biomechanical evaluations to evaluate which group demonstrated better cartilage mechanical resistance to load or cartilage-derived extracellular matrix immunohistochemical staining that may further evaluate cartilage and bone quality were not used in the present cartilage repair analysis. However, full-thickness cartilage defects treated with hDPSCs in a PRP gel scaffold resulted in fewer signs of synovitis, as exhibited by reduced synovial lining cell layer thickening. In addition, enhanced histological cartilage repair was indicated to consist predominantly of hyaline-like cartilage at 12 weeks post-surgery. To conclude, the present results support the therapeutic use of hDPSCs for the treatment of full-thickness articular cartilage defects; however, further studies are warranted.

Acknowledgements

The authors would like to thank Professor Corina da Costa Freitas from the Brazilian National Institute for Space Research (INPE; São José dos Campos, Brazil) for their assistance with statistical analysis. The authors would also like to thank Mr. Milton Alves Junior and Mr. Wilson Orcini for their technical assistance. The present article represents part of the Master's degree thesis project by RHY at Marília Medical School (FAMEMA) in Marília, São Paulo State, Brazil.

Funding

The present study was supported by São Paulo Research Foundation (FAPESP) (grant no. 12/21007-0).

Availability of data and materials

The datasets used and/or analyzed during the current study are available from the corresponding author on reasonable request.

Authors' contributions

RY, RL, SP and LM performed the experiments, analysis and wrote the manuscript; JF, RS, AK, MM, SF and BS generated data and performed analyses; and RS and SP interpreted the data, drafted the manuscript and made critical revisions. All authors discussed the results and reviewed the manuscript.

Ethics approval and consent to participate

The study protocol of the present experiment was reviewed and approved by the Ethics Committee at Faculdade de Medicina de Marília, São Paulo, Brazil (EC No. 641/12).

Patient consent for publication

Not applicable.

Competing interests

The authors declare that they have no competing interests.

References

1. Dominici M, Le Blanc K, Mueller I, Slaper-Cortenbach I, Marini F, Krause D, Deans R, Keating A, Prockop Dj and Horwitz E: Minimal criteria for defining multipotent mesenchymal stromal cells. The international society for cellular therapy position statement. Cytotherapy 8: 315-317, 2006.
2. Steadman JR, Briggs KK, Rodrigo JJ, Kocher MS, Gill TJ and Rodkey WG: Outcomes of microfracture for traumatic chondral defects of the knee: Average 11-year follow-up. Arthroscopy 19: 477-484, 2003.
3. Knutsen G, Drogset JO, Engebretsen L, Grøntvedt T, Isaksen V, Ludvigsen TC, Roberts S, Solheim E, Strand T and Johansen O: A randomized trial comparing autologous chondrocyte implantation with microfracture. Findings at five years. J Bone Joint Surg Am 89: 2105-2112, 2007.
4. Saw KY, Hussin P, Loke SC, Azam M, Chen HC, Tay YG, Low S, Wallin KL and Ragavanaidu K: Articular cartilage regeneration with autologous marrow aspirate and hyaluronic Acid: An experimental study in a goat model. Arthroscopy 25: 1391-1400, 2009.
5. Chen WH, Lo WC, Hsu WC, Wei HJ, Liu HY, Lee CH, Tina Chen SY, Shieh YH, Williams DF and Deng WP: Synergistic anabolic actions of hyaluronic acid and platelet-rich plasma on cartilage regeneration in osteoarthritis therapy. Biomaterials 35: 9599-9607, 2014.
6. Abate M, Verna S, Schiavone C, Di Gregorio P and Salini V: Efficacy and safety profile of a compound composed of platelet-rich plasma and hyaluronic acid in the treatment for knee osteoarthritis (preliminary results). Eur J Orthop Surg Traumatol 25: 1321-1326, 2015.
7. Liu J, Yuan T and Zhang C: Effect of platelet-rich plasma on synovitis of rabbit knee. Zhongguo Xiu Fu Chong Jian Wai Ke Za Zhi 25: 285-290, 2011 (In Chinese).
8. Gotterbarm T, Richter W, Jung M, Berardi Vilei S, Mainil-Varlet P, Yamashita T and Breusch SJ: An in vivo study of a growth-factor enhanced, cell free, two-layered collagen-tricalcium phosphate in deep osteochondral defects. Biomaterials 27: 3387-3395, 2006.
9. Andia I, Sanchez M and Maffulli N: Basic science: Molecular and biological aspects of platelet-rich plasma therapies. Oper Tech Orthop 22: 3-9, 2012.
10. Drengk A, Zapf A, Stürmer EK, Stürmer KM and Frosch KH: Influence of platelet-rich plasma on chondrogenic differentiation and proliferation of chondrocytes and mesenchymal stem cells. Cells Tissues Organs 189: 317-326, 2009.
11. Mishra A, Tummala P, King A, Lee B, Kraus M, Tse V and Jacobs CR: Buffered platelet-rich plasma enhances mesenchymal stem cell proliferation and chondrogenic differentiation. Tissue Eng Part C Methods 15: 431-435, 2009.
12. Akeda K, An HS, Okuma M, Attawia M, Miyamoto K, Thonar EJ, Lenz ME, Sah RL and Masuda K: Platelet-rich plasma stimulates porcine articular chondrocyte proliferation and matrix biosynthesis. Osteoarthritis Cartilage 14: 1272-1280, 2006.
13. Koga H, Muneta T, Nagase T, Nimura A, Ju YJ, Mochizuki T and Sekiya I: Comparison of mesenchymal tissues-derived stem cells for in vivo chondrogenesis: Suitable conditions for cell therapy of cartilage defects in rabbit. Cell Tissue Res 333: 207-215, 2008.
14. Ishizaka R, Hayashi Y, Iohara K, Sugiyama M, Murakami M, Yamamoto T, Fukuta O and Nakashima M: Stimulation of angiogenesis, neurogenesis and regeneration by side population cells from dental pulp. Biomaterials 34: 1888-1897, 2013.
15. Daltoé FP, Mendonça PP, Mantesso A and Deboni MC: Can SHED or DPSCs be used to repair/regenerate non-dental tissues? A systematic review of in vivo studies. Braz Oral Res 28: S1806-83242014000100401, 2014.
16. Jesus AA, Soares MBP, Soares AP, Nogueira RC, Guimarães ET, Araújo TM and Santos RR: Collection and culture of stem cells derived from dental pulp of deciduous teeth: Technique and clinical case report. Dent Press J Orthodont 16: 8, 2011.
17. Sanchez O, Escobar JI and Yunis JJ: A simple G-banding technique. Lancet 2: 269, 1973.
18. Brothman AR, Persons DL and Shaffer LG: Nomenclature evolution: Changes in the ISCN from the 2005 to the 2009 edition. Cytogenet Genome Res 127: 1-4, 2009.
19. Mainil-Varlet P, Aigner T, Brittberg M, Bullough P, Hollander A, Hunziker E, Kandel R, Nehrer S, Pritzker K, Roberts S, *et al*: Histological assessment of cartilage repair: A report by the Histology Endpoint Committee of the international cartilage repair society (ICRS). J Bone Joint Surg Am 85-A (Suppl 2): S45-S57, 2003.
20. van den Borne MP, Raijmakers NJ, Vanlauwe J, Victor J, de Jong SN, Bellemans J and Saris DB; International Cartilage Repair Society: International Cartilage Repair Society (ICRS) and Oswestry macroscopic cartilage evaluation scores validated for use in autologous chondrocyte implantation (ACI) and microfracture. Osteoarthritis Cartilage 15: 1397-1402, 2007.
21. Bonasia DE, Marmotti A, Massa AD, Ferro A, Blonna D, Castoldi F and Rossi R: Intra- and inter-observer reliability of ten major histological scoring systems used for the evaluation of in vivo cartilage repair. Knee Surg Sports Traumatol Arthrosc 23: 2484-2493, 2015.
22. Milano G, Sanna Passino E, Deriu L, Careddu G, Manunta L, Manunta A, Saccomanno MF and Fabbriciani C: The effect of platelet rich plasma combined with microfractures on the treatment of chondral defects: An experimental study in a sheep model. Osteoarthritis Cartilage 18: 971-980, 2010.
23. Krenn V, Morawietz L, Burmester GR, Kinne RW, Mueller-Ladner U, Muller B and Haupl T: Synovitis score: Discrimination between chronic low-grade and high-grade synovitis. Histopathology 49: 358-364, 2006.
24. Yan H and Yu C: Repair of full-thickness cartilage defects with cells of different origin in a rabbit model. Arthroscopy 23: 178-187, 2007.
25. Lee KB, Hui JH, Song IC, Ardany L and Lee EH: Injectable mesenchymal stem cell therapy for large cartilage defects-a porcine model. Stem Cells 25: 2964-2971, 2007.
26. Wakitani S, Goto T, Pineda SJ, Young RG, Mansour JM, Caplan AI and Goldberg VM: Mesenchymal cell-based repair of large, full-thickness defects of articular cartilage. J Bone Joint Surg Am 76: 579-592, 1994.
27. Wakitani S, Imoto K, Yamamoto T, Saito M, Murata N and Yoneda M: Human autologous culture expanded bone marrow mesenchymal cell transplantation for repair of cartilage defects in osteoarthritic knees. Osteoarthritis Cartilage 10: 199-206, 2002.
28. Shao XX, Hutmacher DW, Ho ST, Goh JC and Lee EH: Evaluation of a hybrid scaffold/cell construct in repair of high-load-bearing osteochondral defects in rabbits. Biomaterials 27: 1071-1080, 2006.
29. Andia I, Sánchez M and Maffulli N: Joint pathology and platelet-rich plasma therapies. Expert Opin Biol Ther 12: 7-22, 2012.
30. Olson SA, Horne P, Furman B, Huebner J, Al-Rashid M, Kraus VB and Guilak F: The role of cytokines in posttraumatic arthritis. J Am Acad Orthop Surg 22: 29-37, 2014.
31. E X, Cao Y, Meng H, Qi Y, Du G, Xu J and Bi Z: Dendritic cells of synovium in experimental model of osteoarthritis of rabbits. Cell Physiol Biochem 30: 23-32, 2012.
32. Lories RJ and Luyten FP: The bone-cartilage unit in osteoarthritis. Nat Rev Rheumatol 7: 43-49, 2011.
33. Sakata R, McNary SM, Miyatake K, Lee CA, Van den Bogaerde JM, Marder RA and Reddi AH: Stimulation of the superficial zone protein and lubrication in the articular cartilage by human platelet-rich plasma. Am J Sports Med 43: 1467-1473, 2015.
34. Ando W, Kutcher JJ, Krawetz R, Sen A, Nakamura N, Frank CB and Hart DA: Clonal analysis of synovial fluid stem cells to characterize and identify stable mesenchymal stromal cell/mesenchymal progenitor cell phenotypes in a porcine model: A cell source with enhanced commitment to the chondrogenic lineage. Cytotherapy 16: 776-788, 2014.
35. Jones E and Crawford A: High chondrogenic potential of synovial fluid-derived mesenchymal stromal cells. Cytotherapy 16: 1595-1596, 2014.
36. Rizk A and Rabie AB: Human dental pulp stem cells expressing transforming growth factor β3 transgene for cartilage-like tissue engineering. Cytotherapy 15: 712-725, 2013.
37. Martin-Piedra MA, Garzon I, Oliveira AC, Alfonso-Rodriguez CA, Carriel V, Scionti G and Alaminos M: Cell viability and proliferation capability of long-term human dental pulp stem cell cultures. Cytotherapy 16: 266-277, 2014.
38. Rubio-Azpeitia E and Andia I: Partnership between platelet-rich plasma and mesenchymal stem cells: In vitro experience. Muscles Ligaments Tendons J 4: 52-62, 2014.

39. Abrams GD, Frank RM, Fortier LA and Cole BJ: Platelet-rich plasma for articular cartilage repair. Sports Med Arthrosc 21: 213-219, 2013.
40. Boswell SG, Cole BJ, Sundman EA, Karas V and Fortier LA: Platelet-rich plasma: A milieu of bioactive factors. Arthroscopy 28: 429-439, 2012.
41. Sundman EA, Cole BJ and Fortier LA: Growth factor and catabolic cytokine concentrations are influenced by the cellular composition of platelet-rich plasma. Am J Sports Med 39: 2135-2140, 2011.
42. Carneiro Mde O, Barbieri CH and Barbieri Neto J: Platelet-rich plasma gel promotes regeneration of articular cartilage in knees of sheep. Acta Ortop Bras 21: 80-86, 2013.
43. Serra CI, Soler C, Carillo JM, Sopena JJ, Redondo JI and Cugat R: Effect of autologous platelet-rich plasma on the repair of full-thickness articular defects in rabbits. Knee Surg Sports Traumatol Arthrosc 21: 1730-1736, 2013.
44. Milano G, Deriu L, Sanna Passino E, Masala G, Manunta A, Postacchini R, Saccomanno MF and Fabbriciani C: Repeated platelet concentrate injections enhance reparative response of microfractures in the treatment of chondral defects of the knee: An experimental study in an animal model. Arthroscopy 28: 688-701, 2012.
45. Dohan Ehrenfest DM, Bielecki T, Jimbo R, Barbé G, Del Corso M, Inchingolo F and Sammartino G: Do the fibrin architecture and leukocyte content influence the growth factor release of platelet concentrates? An evidence-based answer comparing a pure platelet-rich plasma (P-PRP) gel and a leukocyte- and platelet-rich fibrin (L-PRF). Curr Pharm Biotechnol 13: 1145-1152, 2012.
46. Pot MW, Gonzales VK, Buma P, IntHout J, van Kuppevelt TH, de Vries RBM and Daamen WF: Improved cartilage regeneration by implantation of acellular biomaterials after bone marrow stimulation: A systematic review and meta-analysis of animal studies. PeerJ 4: e2243, 2016.
47. Shapiro F, Koide S and Glimcher MJ: Cell origin and differentiation in the repair of full-thickness defects of articular cartilage. J Bone Joint Surg Am 75: 532-553, 1993.
48. Wu JP, Kirk TB and Zheng MH: Study of the collagen structure in the superficial zone and physiological state of articular cartilage using a 3D confocal imaging technique. J Orthop Surg Res 3: 29, 2008.
49. Hollander AP, Dickinson SC and Kafienah W: Stem cells and cartilage development: Complexities of a simple tissue. Stem Cells 28: 1992-1996, 2010.